

Bloch-Zener oscillations across a merging transition of Dirac points

Lih-King Lim, Jean-Noël Fuchs and Gilles Montambaux

Laboratoire de Physique des Solides, CNRS UMR 8502, Univ. Paris-Sud, F-91405 Orsay cedex, France.

Bloch oscillations are a powerful tool to investigate spectra with Dirac points. By varying band parameters, Dirac points can be manipulated and merged at a topological transition towards a gapped phase. Under a constant force, a Fermi sea initially in the lower band performs Bloch oscillations and may Zener tunnel to the upper band mostly at the location of the Dirac points. The tunneling probability is computed from the low energy universal Hamiltonian describing the vicinity of the merging. The agreement with a recent experiment on cold atoms in an optical lattice is very good.

PACS numbers: 67.85.Lm, 37.10.Jk, 73.22.Pr, 03.75.Lm, 03.65.Pm

Introduction.— Dirac points in energy bands occur in special two-dimensional (2D) condensed matter systems [1], such as graphene [2], nodal points in d -wave superconductors and surface states of three-dimensional (3D) topological insulators [3]. They are fascinating instances of ultra-relativistic behavior emerging as low-energy effective description of electrons in solids. Dirac points are band touching points that carry a topological charge, namely a Berry phase $\pm\pi$. In most systems, Dirac points occur in dipolar pairs (the so-called fermion doubling). Under variation of external parameters, it is possible to move these Dirac points and even make them merge. This merging signals a topological (Lifshitz) transition between a gapless phase with a disconnected Fermi surface to a gapped phase [4–7]. For example, a uniaxial stress in graphene leads to a motion of the Dirac points but the merging transition is not reachable [8]. The quasi-2D organic conductor α -(BEDT-TTF) $_2$ I $_3$ is a good candidate to observe this transition under pressure [9], however it has not been realized yet.

Recently, a new type of experiment, realized with ultracold atoms loaded in a 2D optical lattice, has provided an alternative way to study Dirac points [10]. By combining techniques of Bloch oscillations and adiabatic mapping of cold atoms, the band structure of the system can be studied with momentum resolution [11–14]. Specifically, the experiment of ETH Zürich [10] utilizes such techniques for a non-interacting Fermi gas in a tunable two-band system featuring Dirac points. Their existence is revealed through Landau-Zener (LZ) tunneling from the lower to the upper band. As the lattice amplitude is varied, a drastic change in the transferred atomic fraction provides a qualitative signature of the Dirac points and their merging.

In this letter, we present a complete description of Landau-Zener tunneling through a pair of Dirac points, using a universal low-energy Hamiltonian describing the merging transition [7]. We show how the transferred fraction provides a key signature of the merging transition and that it depends crucially on the direction of the motion with respect to the merging direction. We find a very good agreement between the computed aver-

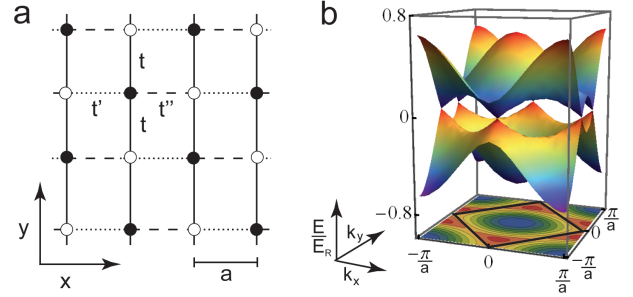


FIG. 1: (color online). (a) Square lattice indicating the hopping amplitudes and the two inequivalent sites. (b) Band structure in the gapless D phase for $t' = t = 0.2$, $t'' = 0.05$ in units of E_R , see text. The first Brillouin zone is indicated by the square.

aged LZ probabilities and the experimental data. Furthermore, new experimental signatures for varying Bloch oscillations and a coherent Stückelberg interferometry are presented.

Tight-binding model.— We consider a nearest-neighbor tight-binding model on a square lattice. The four hopping amplitudes between neighbors are taken as t, t along y - and t', t'' along x -direction (see Fig. 1). When $t' \neq t''$, there are two inequivalent sites – called A and B – per unit cell giving rise to two bands. When $t'' = 0$, a link is broken realizing a brick-wall lattice, which has the same connectivity as the honeycomb lattice albeit with a rectangular geometry. When $t' = t''$, it is a standard square lattice with anisotropic amplitudes along x and y and a single site per unit cell. The Hamiltonian (with nearest neighbor distance $a \equiv 1$ and $\hbar \equiv 1$) reads

$$H = \begin{pmatrix} 0 & f(\mathbf{k}) \\ f^*(\mathbf{k}) & 0 \end{pmatrix} \quad (1)$$

with $f(\mathbf{k}) = -(te^{ik_y} + te^{-ik_y} + t'e^{ik_x} + t''e^{-ik_x})$ where the hopping amplitudes are positive and $\mathbf{k} = (k_x, k_y)$ is the Bloch wavevector. The energy spectrum is given by $\epsilon(\mathbf{k}) = \pm|f(\mathbf{k})|$. It features two Dirac cones when $t' + t'' < 2t$ (gapless D phase) and a gap when $t' + t'' > 2t$

(gapped G phase). At $t' + t'' = 2t$ the Dirac points merge at $\mathbf{k} = (0, \pi)$ and there is a single touching point between the two bands. When $t' = t''$, the band structure is that of a square lattice, with lines of Dirac points (L phase), which becomes isotropic when $t' = t'' = t$ (I phase). This model can therefore describe the transition between the G and D phase, and moreover, the crossover from the D to L phase. In the following, energies are measured in units of the recoil energy $E_R = \pi^2 \hbar^2 / (2ma^2)$ where m is the atomic mass.

Mapping to the universal Hamiltonian.— In a crystal which is time-reversal and inversion symmetric, merging can only occur at $\mathbf{G}/2$ points where \mathbf{G} is a reciprocal lattice vector. Near such a point, it is possible to write a minimal low energy Hamiltonian that captures the topological transition and describes both Dirac cones at once [7]. Close to the merging, an expansion for small $\mathbf{q} = \mathbf{k} - \mathbf{G}/2$ gives rise to an effective Hamiltonian which has the universal form

$$\mathcal{H} = \begin{pmatrix} 0 & \Delta_* + \frac{q_y^2}{2m^*} - ic_x q_x \\ \Delta_* + \frac{q_y^2}{2m^*} + ic_x q_x & 0 \end{pmatrix} \quad (2)$$

and a spectrum $\epsilon = \pm \sqrt{(\frac{q_y^2}{2m^*} + \Delta_*)^2 + c_x^2 q_x^2}$. The model depends on three independent parameters Δ_* , m^* and c_x . The merging transition is driven by the parameter Δ_* hereafter called the merging gap. When $\Delta_* < 0$, the spectrum contains two Dirac points at $\mathbf{q}_D = (0, \pm \sqrt{2m^*|\Delta_*|})$ and $|\Delta_*|$ represents the energy of the saddle points connecting them, which is located at $\mathbf{q} = 0$ (D phase). When increasing Δ_* towards 0, the two Dirac points approach each other along the q_y direction until they merge when $\Delta_* = 0$. Exactly at the merging, there is a single touching point between the two bands, with a semi-Dirac (or hybrid) spectrum $\epsilon = \pm \sqrt{(q_y^2/2m^*)^2 + (c_x q_x)^2}$ [5, 15]. By increasing the driving parameter still further, a true gap of magnitude $2\Delta_* > 0$ opens at $\mathbf{q} = 0$ (G phase). We map the tight-binding to the universal model by comparing their energy expansions near the Dirac points [7]. In the D phase, we find $\Delta_* = t' + t'' - 2t$ and the Dirac cone velocities are $c_x = t' - t''$ and $c_y = \sqrt{4t^2 - (t' + t'')^2}$, so that the mass is obtained from $m^* = -2\Delta_*/c_y^2 = 2/(2t + t' + t'')$. In the G phase, Δ_* and c_x are unchanged and $m^* = 1/(2t)$.

Landau-Zener tunneling with Dirac cones.— Consider atoms initially in the lower band performing Bloch oscillations under the influence of a constant applied force F . By accelerating these atoms in the vicinity of a Dirac point, their tunneling probability to the upper band is finite, a problem considered by Landau and Zener [16]. In the following, the universal low-energy Hamiltonian is used to compute the interband transition probability.

Motion along the k_x direction: single Dirac cone.— In the D phase, an atom moving along the k_x direction encounters at most one Dirac cone during a single Bloch

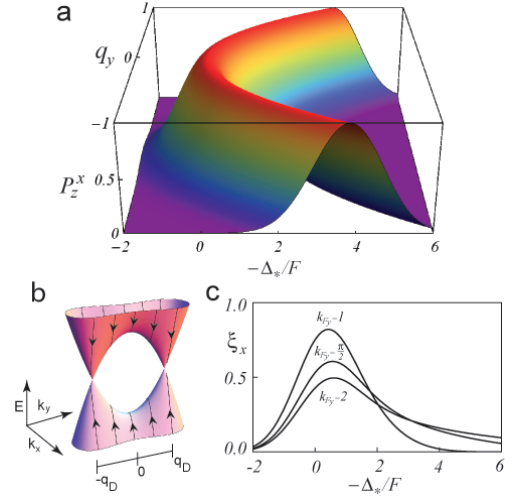


FIG. 2: (color online). *Motion along k_x .* (a) LZ probability P_Z^x (eq. (3)) as a function of $-\Delta_*/F$ and of the transverse momentum q_y . Here $c_x/F \approx 0.5$ and $m^*F \approx 0.13$. (b) Trajectories along the k_x direction. (c) Transferred fraction to the upper band ξ_x as a function of $-\Delta_*/F$ for different sizes k_{Fy} of the cloud.

oscillation (Fig. 2b). The LZ probability for such a linear avoided band crossing is given by [16]

$$P_Z^x = e^{-\pi \frac{(\text{gap}/2)^2}{c_x F}} = e^{-\pi \frac{(\frac{q_y^2}{2m^*} + \Delta_*)^2}{c_x F}} \quad (3)$$

where q_y is the position with respect to the merging point $\mathbf{G}/2 = (0, \pi)$. Note that $P_Z^x = 1$ for $q_y = \pm q_D = \pm \sqrt{-2m^*\Delta_*}$, positions of the two Dirac points. Actually Eq. (3) is not only valid in the D but extends to the G phase across the merging transition. This quantity is shown in Fig. 2a as a function of the transverse momentum q_y and Δ_* .

As the experiment is performed with a cloud of non-interacting fermions, we need also to average the LZ probability over the initial distribution of atoms. We consider a 2D cloud of harmonically trapped fermions at zero temperature for a filling fraction sufficiently smaller than half-filling. The energy spectrum close to $\mathbf{k} = 0$ is $\epsilon(\mathbf{k}) \approx k_x^2/(2m_x) + k_y^2/(2m_y)$ (as measured from the band bottom) with the band masses $m_x = (2t + t' + t'')/[4t't'' + 2t(t' + t'')]$ and $m_y = 1/(2t)$. The semiclassical energy of an atom is therefore $\epsilon(\mathbf{k}, \mathbf{r}) = k_x^2/(2m_x) + k_y^2/(2m_y) + (m_x \omega_x x^2 + m_y \omega_y^2 y^2)/2$ where $\omega_x/2\pi$ and $\omega_y/2\pi$ are the trapping frequencies [17]. The fraction ξ_x of atoms transferred to the upper band is then given by the averaged probability $\xi_x = \langle P_Z^x \rangle$ where

$$\langle \dots \rangle = \frac{\int_{\epsilon(\mathbf{k}, \mathbf{r}) < \epsilon_F} dk_x dk_y dx dy \dots}{\int_{\epsilon(\mathbf{k}, \mathbf{r}) < \epsilon_F} dk_x dk_y dx dy} \quad (4)$$

and $\epsilon_F = k_{Fx}^2/(2m_x) = k_{Fy}^2/(2m_y)$ is the Fermi energy,

which defines k_{Fx} and k_{Fy} [18]. The transferred fraction

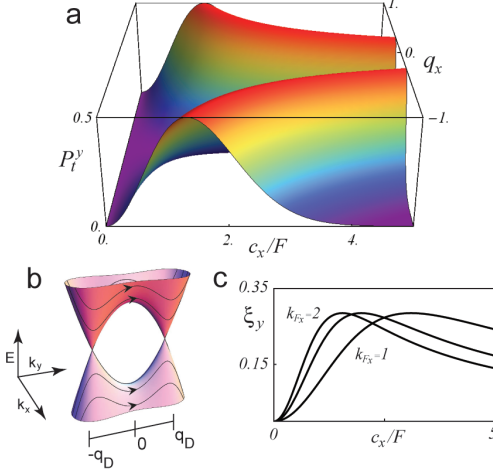


FIG. 3: (color online). *Motion along k_y .* (a) Total probability P_t^y for atoms tunneling to the upper band (eq. (6)) as a function of c_x/F and of the transverse momentum q_x . Here $\Delta_*/F = -5$ and $m^*F \approx 0.13$. (b) Double LZ tunneling along the k_y direction. (c) Transferred fraction ξ_y as a function of c_x/F for various sizes k_{Fx} of the initial cloud.

ξ_x as a function of Δ_* and of the size k_{Fy} of the cloud is shown in Fig. 2c. For a cloud of finite size k_{Fy} , only a finite proportion of atoms may tunnel to the upper band when $\Delta_* < 0$.

Motion along the k_y direction: double Dirac cone.— In the G phase, the tunneling probability is vanishingly small. In the following, we concentrate on the D phase where atoms performing one Bloch oscillation in the k_y direction have the possibility to encounter two inequivalent Dirac cones successively. The scenario is therefore richer than before since the tunneling process implies two successive Landau-Zener events (see Fig. 3b). The probability P_Z^y associated with each LZ event is now

$$P_Z^y \equiv e^{-2\pi\delta} = e^{-\pi \frac{c_x^2 q_x^2}{c_y F}} = e^{-\pi \frac{c_x^2 q_x^2}{F \sqrt{2} |\Delta_*|/m^*}} \quad (5)$$

which defines the adiabaticity parameter δ . In the following, we calculate the total interband probability P_t^y associated with the two successive events, in the limit where they can be considered independent. Quantitatively, the LZ tunneling time $\sim \max(\sqrt{\delta}, \delta)/c_x q_x$ [19] should be shorter than the time $2\sqrt{2m^*|\Delta_*|}/F$ it takes an atom to travel between the two Dirac points, i.e. not too close to the merging transition.

First assuming that the two tunneling events are incoherent, we combine the probabilities to find the interband transition probability [18, 19]

$$P_t^y = 2P_Z^y(1 - P_Z^y) \quad (6)$$

which is shown in Fig. 3a as a function of c_x and the transverse momentum q_x . Notice that P_t^y vanishes when $q_x = 0$ because $P_Z^y = 1$. For an initial cloud of size k_{Fx} , the transferred fraction is $\xi_y = \langle P_t^y \rangle$ where the average is defined in Eq. (A.6) [18]. The result is shown in Fig. 3c.

Comparison to the experiment.— The ETH experiment is performed on a harmonically trapped 3D Fermi gas loaded in a 2D optical trap [10]. Our model treats a trapped 2D Fermi gas in a 2D band structure. The optical lattice potential is $V(x, y) = -V_{\bar{X}} \cos^2(\pi x + \theta/2) - V_X \cos^2(\pi x) - V_Y \cos^2(\pi y) - 2\alpha\sqrt{V_X V_Y} \cos(\pi x) \cos(\pi y)$, where $\alpha = 0.9$, $\theta = \pi$, and the laser wavelength is $2a$ with amplitudes $V_Y = 1.8$, $0 \leq V_{\bar{X}} \leq 6.5$ and $0 \leq V_X \leq 1$. To make a precise comparison, we perform single-particle numerical band structure calculation provided by the 2D optical potential using a truncated plane-wave expansion, and establish a map between the optical lattice parameters and that of the universal Hamiltonian of Eq. (2) for $\Delta_* < 0$. The latter is done by fitting the parameters of the universal Hamiltonian to the two lowest lying energy bands in the vicinity of the Dirac cones [18]. The corresponding (t, t', t'') -tight-binding model is then obtained by the analytical mapping (see paragraph after Eq. (2)) — the main features that are not captured are the Dirac cones tilting and the particle-hole asymmetry, which appear not to be relevant. Qualitatively, t stays roughly constant in the considered range of optical lattice parameters. The hopping t' increases when $V_X - V_{\bar{X}}$ increases, whereas t'' increases when $V_X + V_{\bar{X}}$ decreases. Finally we compute the transferred fractions ξ_x and ξ_y as a function of V_X and $V_{\bar{X}}$, shown in Fig. 4. For the experimental parameters $F = 0.02$, $k_{Fy} \simeq \pi/2$ and $k_{Fx} \simeq 2$ (corresponding to $\epsilon_F \approx 0.4$), we find a striking agreement with Figs. 4a and 4b of Ref. [10].

Discussion.— First consider the case of the motion along k_x . The line of maximum transfer probability ξ_x (red region in Fig. 4a) corresponds to a maximal LZ probability $P_Z^x \approx 1$ for a large number of atoms. Playing with the averaging order gives $\xi_x \approx \exp[-\pi \langle (q_y^2/2m^* + \Delta_*)^2 \rangle / (c_x F)]$, in which $\langle q_y^2 \rangle = k_{Fy}^2/6$ and $\langle q_y^4 \rangle = k_{Fy}^4/16$. Its maximum occurs when $\Delta_* \simeq -\langle q_y^2 \rangle / (2m^*)$, which explains why it is near the merging line $\Delta_* = 0$, but slightly inside the D phase, as seen experimentally. The transferred fraction ξ_x is a symmetric function of its natural variable Δ_* — when doing the average properly it is actually slightly asymmetric — and its width reduces when decreasing c_x (by decreasing V_X). Both features are seen experimentally, see Fig. 4a of Ref. [10]. Obviously, the width and the maximum should increase when increasing F .

Adding a staggered on-site potential $\pm\Delta/2$ opens a gap Δ in the spectrum. Experimentally, this gap is controlled by the parameter θ of the potential $V(x, y)$. It was found that the decay of the transferred fraction ξ_x as a function of θ is well fitted by a gaussian (see Fig. 2b of Ref.

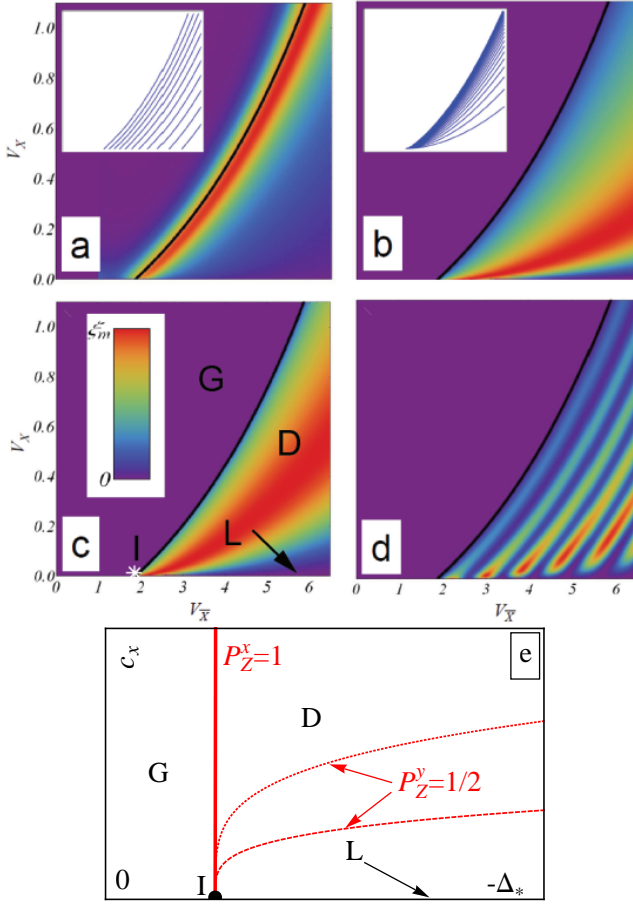


FIG. 4: (color online). a) Transferred fraction ξ_x as a function of the optical lattice parameters $V_{\bar{x}}$ and V_x (here $k_{Fy} = \pi/2$, $F = 0.02$). Inset: lines of constant Δ_* . b) Transferred fraction ξ_y ($k_{Fx} = 2$, $F = 0.02$). Inset: lines of constant c_x^2/c_y . c) Same as (b) with $F = 0.1$. d) Same parameters as (b) taking coherence into account and leading to Stückelberg oscillations. e) Phase diagram in the $(-\Delta_*, c_x)$ plane showing the G, D, L, and I phases (see text). $P_Z^x = 1$ along the merging transition (continuous line). The crossover line $P_Z^y = 1/2$ corresponds to $c_x \propto F^{1/2}|\Delta_*|^{1/4}$ and is plotted for two different forces (dashed and dotted lines). The color code for (a)-(d) is such that $\xi_m = 0.5, 0.3, 0.3$, and 0.6 , respectively. The black line in (a)-(d) indicates the merging transition $\Delta_* = 0$.

[10]). Here, we prove that it is of the form $\xi_x(\Delta) = \xi_x(0) \exp(-\pi\Delta^2/(4c_x F))$ and that $\Delta \approx 4.3(\theta/\pi - 1)$ for the experimental parameters $V_{\bar{x},X,Y} = [3.6, 0.28, 1.8]$.

Next, consider the case of the motion along k_y . The interband transition probability (Eq. 6) is a non monotonous function of the LZ probability P_Z^y and it is maximum when $P_Z^y = 1/2$. This explains the existence of the maximum of ξ_y well *inside* the D phase (red region in Fig. 4b). When playing with the averaging order, $\xi_y \approx e^{-X}(1 - e^{-X})/2$ where $X \equiv \pi c_x^2 \langle q_x^2 \rangle / c_y F$. The maximum occurs when $e^{-X} \approx 1/2$ i.e. when

$c_x^2/c_y \simeq F \ln 2 / (\pi \langle q_x^2 \rangle) = \text{const.}$ Compared to the previous case, ξ_y is a much more asymmetric function of its natural variable $X \propto c_x^2/c_y$: the decay at large X is slower than at small X (the signal extends more towards large c_x , which is seen experimentally). In contrast to the previous case, the position of the line of maxima depends on F , as shown in Figs. 4b and 4c, but its amplitude is almost independent. Its width decreases when $c_x \rightarrow 0$. Furthermore, ξ_y vanishes as $V_x \rightarrow 0$, eventually reaching the square lattice limit (L phase).

Since the two LZ events along k_y are expected to be coherent, Stückelberg interferences in the transferred fraction ξ_y should be observable. Eq. (6) should indeed be replaced by $P_t^y = 4P_Z^y(1 - P_Z^y) \cos^2(\varphi/2 + \varphi_d)$ where $\varphi = 4 \int_0^{q_D} dq_y \sqrt{(\Delta_* + q_y^2/2m^*)^2 + c_x^2 q_x^2 / F}$ is a dynamically acquired phase in between the two tunneling events and $\varphi_d = -\pi/4 + \delta(\ln \delta - 1) + \arg \Gamma(1 - i\delta)$ is a phase delay given in terms of the gamma function and δ is defined in Eq. (5) [18, 19]. Averaging P_t^y over the 2D atomic distribution gives the transferred fraction ξ_y shown in Fig. 4d. However, such interferences are not observed in the ETH experiment, which we attribute to averaging over the third spatial direction. Briefly, interference fringes in Fig. 4d are lines of constant Δ_* with a fringe spacing $\sim 0.04 E_R$. For the experimentally given trapping frequency in the z direction, we estimate that Δ_* varies along z by $\sim 0.03 E_R$. This should be enough to wash out the interferences.

Conclusion.— Landau-Zener tunneling conveniently probes the energy spectrum in the vicinity of Dirac points. Depending on the direction of the applied force, the atoms experience a LZ transition through a single or a pair of Dirac cones. We calculated the transferred fraction in the framework of the universal Hamiltonian describing the merging transition, and found a very good agreement with the ETH experiment. To summarize, the important parameters are the merging gap Δ_* and the velocity c_x perpendicular to the merging direction. A simplified phase diagram is shown in Fig. 4e. Although the transfer through a single Dirac cone probes the merging transition, the transfer through a pair of cones signals a double Landau-Zener event inside the D phase and a cross-over towards the L phase.

As perspectives, we expect Stückelberg interferences to be observable in the strictly 2D regime. Furthermore, it should now be possible to tune the optical lattice right at the merging transition and to study the semi-Dirac spectrum, thus opening the way to explore new phenomena. For example, applying an artificial $U(1)$ gauge potential [20, 21] should reveal unusual Landau levels [5].

We acknowledge support from the Nanosim Graphene project under grant number ANR-09-NANO-016-01.

- [2] A. H. Castro Neto *et al.*, Rev. Mod. Phys. **81**, 109 (2009).
- [3] M. Z. Hasan and C. L. Kane, Rev. Mod. Phys. **82**, 3045 (2010).
- [4] Y. Hasegawa *et al.*, Phys. Rev. B **74**, 033413 (2006).
- [5] P. Dietl *et al.*, Phys. Rev. Lett. **100**, 236405 (2008).
- [6] B. Wunsch *et al.*, New J. Phys. **10**, 103027 (2008).
- [7] G. Montambaux *et al.*, Phys. Rev. B **80**, 153412 (2009); Eur. Phys. J. B **72**, 509 (2009).
- [8] V.M. Pereira *et al.*, Phys. Rev. B **80**, 045401 (2009); M. O. Goerbig *et al.*, Phys. Rev. B **78**, 045415 (2008).
- [9] S. Katayama *et al.*, J. Phys. Soc. Jap. **75**, 054705 (2006).
- [10] L. Tarruell *et al.*, arXiv:1111.5020 (2011).
- [11] O. Morsch and M. Oberthaler, Rev. Mod. Phys. **78**, 179 (2006).
- [12] T. Salger *et al.*, Phys. Rev. Lett. **99**, 190405 (2007).
- [13] S. Kling *et al.*, Phys. Rev. Lett. **105**, 215301 (2010).
- [14] M. Ölschläger *et al.*, Phys. Rev. Lett. **108**, 075302 (2012).
- [15] V. Pardo and W.E. Pickett, Phys. Rev. Lett. **102**, 166803 (2009).
- [16] L.D. Landau, Phys. Z. Sow. **2**, 46 (1932); C. Zener, Proc. R. Soc. London A **137**, 696 (1932); see also C. Wittig, J. Phys. Chem. B **109**, 8428 (2005).
- [17] Trapping frequencies were measured from dipole oscillations in the optical lattice [10]. Therefore the band masses replace the bare masses in the harmonic potential energy.
- [18] See Supplemental Material.
- [19] S.N. Shevchenko *et al.*, Phys. Rep. **492**, 1 (2010).
- [20] J. Dalibard, F. Gerbier, G. Juzeliūnas, and P. Öhberg, Rev. Mod. Phys. **83**, 1523 (2011).
- [21] M. Aidelsburger, M. Atala, S. Nascimbène, S. Trotzky, Y.-A. Chen, and I. Bloch, Phys. Rev. Lett. **107**, 255301 (2011).

Appendix

NUMERICAL BAND STRUCTURE CALCULATION

In the experiment [A1], a 2D tunable optical potential of the form

$$\begin{aligned}
 V(x, y) = & -V_{\bar{X}} \cos^2(kx + \theta/2) - V_X \cos^2(kx) \\
 & -V_Y \cos^2(ky) - 2\alpha\sqrt{V_X V_Y} \cos(kx) \\
 & \times \cos(ky) \cos(\varphi)
 \end{aligned} \tag{A.1}$$

is utilized. Here, $V_{\bar{X}}$, V_X and V_Y are proportional to the tunable laser intensities, $\alpha = 0.9$ is the visibility of the interference pattern, and other parameters $\theta = \pi, \varphi = 0$ are fixed for the most part in the experiment. $k = 2\pi/\lambda$ is the laser wave vector, and the nearest neighbor lattice distance used in the main text $a = \lambda/2$. The Bravais lattice of the optical potential is given by $\mathbf{a}_1 = (\lambda/2)(1, -1)$, $\mathbf{a}_2 = (\lambda/2)(1, 1)$, and the corresponding reciprocal vector is given as $\mathbf{b}_1 = (2\pi/\lambda)(1, -1)$, $\mathbf{b}_2 = (2\pi/\lambda)(1, 1)$. The single-particle bandstructure is obtained by numerically solving the 2D Schrödinger equation

$$\left[-\frac{\hbar^2}{2m_0} \Delta + V(\mathbf{r}) \right] \psi(\mathbf{r}) = E\psi(\mathbf{r}). \tag{A.2}$$

By writing the wavefunction in Bloch's form $\psi_{\mathbf{k}}(\mathbf{r}) = \exp(i\mathbf{k} \cdot \mathbf{r}) \sum_{m,n \in \mathbb{Z}} u(m, n) \exp(im\mathbf{b}_1 \cdot \mathbf{r} + in\mathbf{b}_2 \cdot \mathbf{r})$, the Schrödinger equation in terms of the Fourier components $u(m, n)$ becomes

$$\begin{aligned}
 & \left\{ \frac{\hbar^2}{2m_0} [(k_x + 2\pi(m+n)/\lambda)^2 + (k_y + 2\pi(m-n)/\lambda)^2] \right. \\
 & + \delta_1 \} u(m, n) + \{ \delta_2 u(m-1, n-1) + \delta_3 u(m-1, n) \\
 & + \delta_4 u(m-1, n+1) + \delta_3 u(m, n-1) + \delta_3 u(m, n+1) \\
 & + \delta_4 u(m+1, n-1) + \delta_3 u(m+1, n) \\
 & \left. + \delta_2 u(m+1, n+1) \right\} = E u(m, n),
 \end{aligned} \tag{A.3}$$

where the various constants are defined as $\delta_1 = -(V_{\bar{X}} + V_X - V_Y)/2$, $\delta_2 = (V_{\bar{X}} - V_X)/4$, $\delta_3 = -0.45\sqrt{V_X V_Y}$ and $\delta_4 = V_Y/4$. We truncate the Fourier coefficients $u(m, n)$ at $|m|, |n| = 2$ and solve the resulting 25 secular equations in *Mathematica* to obtain the discrete energy bands $E_i(\mathbf{k})$ for each \mathbf{k} . A convergence test has been carried out for the numerical bandstructure calculation up to a truncation at $|m|, |n| = 3$, which yields an excellent agreement with the $|m|, |n| = 2$ case.

A typical bandstructure for a particular set of laser amplitudes is shown in Fig. A1(a), in the convenient recoil energy unit $E_R = \hbar^2/2m_0\lambda^2$ where m_0 is the atomic mass. From the two lowest bands, see Fig. A1(b), we then determine the magnitude of the gap Δ_* , the distance between the two Dirac points q_D and the slope c_x

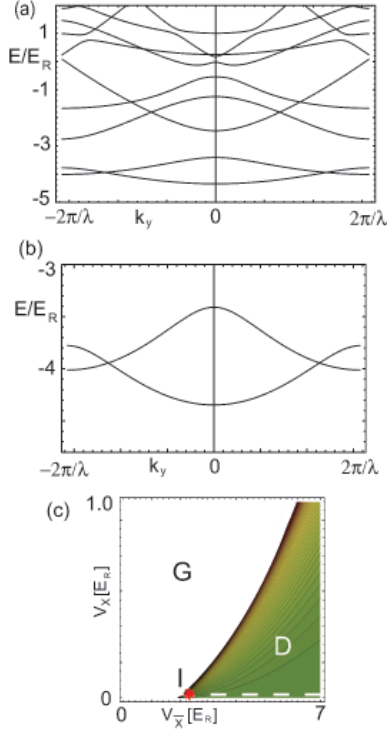


FIG. A1: (a) Bandstructure for $V_{\bar{X}} = 5 E_R$, $V_X = 0.3 E_R$, $V_Y = 1.8 E_R$ in the k_y -direction with $k_x = 0$. (b) The two lowest bands featuring two inequivalent Dirac points. (c) The three phases D , G and L (dashed line) realized with the optical potential. The starred point indicates the position where the isotropic square lattice model (I phase) is realized.

around the Dirac points in the x direction as a function of $V_{\bar{X}}$ and V_X , for a fixed $V_Y = 1.8 E_R$. The interpolation formulae in the gapless phase are obtained as follow:

$$\begin{aligned}
 |\Delta_*(V_{\bar{X}}, V_X)| &= (0.1134 + 0.0218 V_X - 0.0205 V_X^2) \\
 &\times \ln[1 + (V_{\bar{X}} - 3.8234 \ln[2.7560 V_X + 1.6325])^{1.2}], \\
 q_D(V_{\bar{X}}, V_X) &= (0.65 + 0.1 V_X) \\
 &\times (V_{\bar{X}} - 3.8234 \ln[2.7560 V_X + 1.6325])^{0.42+0.05 V_X}, \\
 c_x(V_{\bar{X}}, V_X) &= 1.1204 e^{-0.3023 V_{\bar{X}}} \\
 &\times V_X^{0.3791 \ln[1.8380 V_{\bar{X}} - 0.7251]}. \tag{A.4}
 \end{aligned}$$

The slope in the y -direction around a Dirac cone is then given by $c_y = 2|\Delta_*|/q_D$. Furthermore, the boundary between the gapped and the gapless phase is given by

$$V_{\bar{X}} = a_1 \ln[a_2 V_X + a_3] \tag{A.5}$$

with $a_1 = 3.8234$, $a_2 = 2.7360$, $a_3 = 1.6325$. After translating into the more intuitive anisotropic square lattice model with t, t', t'' hopping amplitudes (see the paragraph after Eqn (2) in the main text), we then locate the various phases that are realized as a function of the laser amplitudes, see Fig. A1(c).

AVERAGING OVER THE ATOMIC DISTRIBUTION

Motion along the k_x direction: single Dirac cone

As the experiment is done with a cloud of non-interacting Fermi gas, we need to average the Landau-Zener probability over the distribution of atoms. Taking a 2D cloud of harmonically trapped atoms at zero temperature filled up to the Fermi energy ϵ_F (measured from the band bottom), the fraction of atoms transferred to the upper band is given by the averaged tunneling probability $\langle P_Z^x \rangle$ where the average is defined as

$$\langle \dots \rangle = \frac{\int_{\epsilon(\mathbf{k}, \mathbf{r}) < \epsilon_F} dk_x dk_y dx dy \dots}{\int_{\epsilon(\mathbf{k}, \mathbf{r}) < \epsilon_F} dk_x dk_y dx dy} \tag{A.6}$$

Since the low energy expansion of the spectrum $\epsilon(\mathbf{k})$ associated with the tight-binding Hamiltonian (1) is $\epsilon(\mathbf{k}) = tt'k_x^2/(2t+t') + tk_y^2$ (as measured from the band bottom), the semiclassical energy of an atom in the 2D anisotropic harmonic oscillator is $\epsilon(\mathbf{k}, \mathbf{r}) = \frac{k_x^2}{2m_x} + \frac{k_y^2}{2m_y} + \frac{1}{2}(m_x \omega_x x^2 + m_y \omega_y^2 y^2)$, where $m_x = (2t+t')/(2tt')$ and $m_y = 1/(2t)$ are the band masses and $\omega_x/2\pi$ and $\omega_y/2\pi$ the trapping frequencies [A2], the average is given by

$$\langle \dots \rangle = \frac{16}{3\pi k_{Fy}^4} \int_0^{k_{Fy}} dk_y (k_{Fy}^2 - k_y^2)^{3/2} \dots \tag{A.7}$$

where $\epsilon_F \equiv \frac{k_{Fy}^2}{2m_y} = \frac{k_x^2}{2m_x} + \frac{k_y^2}{2m_y} + \frac{1}{2}(m_x \omega_x x^2 + m_y \omega_y^2 y^2)$ defines the 2D Fermi surface.

Motion along the k_y direction: double Dirac cone

For an initial cloud of size k_{Fx} , the transferred fraction is $\langle P_t^y \rangle$ where the average is defined in (A.6) and becomes

$$\langle \dots \rangle = \frac{16}{3\pi k_{Fx}^4} \int_0^{k_{Fx}} dk_x (k_{Fx}^2 - k_x^2)^{3/2} \dots \tag{A.8}$$

where $k_{Fx} \equiv \sqrt{2m_x \epsilon_F}$.

STÜCKELBERG OSCILLATIONS

In the following, we calculate the total inter-band probability associated to the two successive LZ events, in the limit where they can be considered to be separated. This is the case if the system is in the D phase and not too close to the merging. Quantitatively, the Zener tunneling time [A3] $\tau \sim \max(\sqrt{\delta}, \delta)/c_x q_x$ should be shorter than the time $T = 2q_D/F = 2\sqrt{2m_*}|\Delta_*|/F$ it takes to travel between the two Dirac points, where $\delta = c_x^2 q_x^2/(2c_y F)$ is the adiabaticity parameter.

If the sequence between the two tunneling events is coherent, amplitudes have to be considered instead of probabilities, effectively realizing a coherent Stückelberg interferometer [A3]. In this case, the total probability amplitude to go from the lower to the upper band is the sum of the amplitude for two distinct paths. In path 1, the atom jumps to the upper band at the first avoided band crossing (Dirac cone) and then stays in the upper band at the second, such that the amplitude is $A_1 = \sqrt{P_Z^y} e^{i\varphi_d} \times e^{i\varphi_1} \times \sqrt{1 - P_Z^y}$ where $\sqrt{P_Z^y} e^{i\varphi_d}$ is the amplitude to jump at a single avoided band crossing – the associated probability of a single LZ event being P_Z^y – and $\varphi_1 = \int_0^T dt E_{\text{upper band}}(t)$ is the phase dynamically acquired by the atom traveling in the upper band between the two Dirac cones. The phase delay φ_d which is accumulated at each tunneling event is given by $\varphi_d = -\pi/4 + \delta(\ln \delta - 1) + \arg \Gamma(1 - i\delta)$ where $\Gamma(z)$ is the gamma function [A3]. Up to a $\pi/2$ shift, this phase is the so-called Stokes phase. In path 2, the atom stays in the lower band at the first Dirac cone and then jumps to the upper band at the second. The associated amplitude is $A_2 = \sqrt{1 - P_Z^y} \times e^{i\varphi_2} \times \sqrt{P_Z^y} e^{-i\varphi_d}$ where $\varphi_2 = \int_0^T dt E_{\text{lower band}}(t)$ is the dynamically acquired phase of the atom traveling in the lower band from one Dirac cone to the other. The total probability is therefore

$$P_t^y = |A_1 + A_2|^2 = 4P_Z^y(1 - P_Z^y) \cos^2(\varphi/2 + \varphi_d) \quad (\text{A.9})$$

where $\varphi = \varphi_1 - \varphi_2$ is the dynamically accumulated phase between the two tunneling events

$$\varphi = \int_0^T \Delta E(t) dt = \frac{1}{F} \int_{-q_D}^{q_D} \Delta E(q_y) dq_y \quad (\text{A.10})$$

with $\Delta E \equiv E_{\text{upper band}} - E_{\text{lower band}}$. For the universal Hamiltonian, we have

$$\varphi = \frac{4}{F} \int_0^{\sqrt{2m^*|\Delta_*|}} dq_y \sqrt{\left(\frac{q_y^2}{2m^*} + \Delta_*\right)^2 + c_x^2 q_x^2} \quad (\text{A.11})$$

which can be written in the form

$$\varphi = 4\sqrt{2m^*} \frac{|\Delta_*|^{3/2}}{F} I\left(\frac{c_x q_x}{|\Delta_*|}\right) \quad (\text{A.12})$$

where the function $I(x)$ is given by $I(x) = \int_0^1 du \sqrt{(u^2 - 1)^2 + x^2}$ and well approximated by $I(x) \approx \sqrt{4/9 + x^2}$. From Eq. (A.9), the incoherent limit (Eq. (6) in the main text) is easily recovered by averaging over the phase.

-
- [A1] L. Tarruell, D. Greif, T. Uehlinger, G. Jotzu and T. Esslinger, arXiv:1111.5020 .
- [A2] The trapping frequencies were measured from dipole oscillations in presence of the optical lattice, therefore it is the band masses that appear in the harmonic potential energy and not the bare atomic masses.
- [A3] S.N. Shevchenko, S. Ashhab, F. Nori, Phys. Rep. **492**, 1 (2010).